



## Avalanches in strong imbibition

Bauyrzhan K. Primkulov <sup>1</sup>, Benzhong Zhao <sup>2</sup>, Christopher W. MacMinn <sup>3</sup> & Ruben Juanes <sup>1</sup>✉

Slow injection of non-wetting fluids (drainage) and strongly wetting fluids (strong imbibition) into porous media are two contrasting processes in many respects: the former must be forced into the pore space, while the latter imbibe spontaneously; the former occupy pore bodies, while the latter coat crevices and corners. These two processes also produce distinctly different displacement patterns. However, both processes evolve via a series of avalanche-like invasion events punctuated by quiescent periods. Here, we show that, despite their mechanistic differences, avalanches in strong imbibition exhibit all the features of self-organized criticality previously documented for drainage, including the correlation scaling describing the space-time statistics of invasion at the pore scale.

<sup>1</sup>Massachusetts Institute of Technology, 77 Massachusetts Avenue, Cambridge, MA, USA. <sup>2</sup>McMaster University, 1280 Main Street West, Hamilton, ON, Canada. <sup>3</sup>University of Oxford, Parks Road, Oxford, UK. ✉email: [juanes@mit.edu](mailto:juanes@mit.edu)

The complexity of the world around us—in rivers, climate patterns, landslides, and earthquakes—is often attributed to the prevalence of self-organized criticality (SOC), where systems naturally evolve toward a state in which small perturbations have scale-free consequences<sup>1</sup>. Slow injection of a non-wetting fluid (i.e. slow drainage, Fig. 1a–c) into a porous medium is arguably one of the most accessible examples of SOC<sup>2–7</sup>. It can be studied in great detail with benchtop experiments and simple pore-network models<sup>6–8</sup>, and the universality of observed trends can be tested by changing the properties of the fluids and the porous medium<sup>9</sup>.

In drainage, constant-rate displacement is achieved by forcing the invading fluid into the porous medium. In slow drainage, when viscous forces are negligible, the invading fluid advances into clusters of pore bodies via intermittent avalanches<sup>10,11</sup>, with waiting times between events and sizes of invasion clusters exhibiting scale-free behavior<sup>6</sup>. These scale-free features are the hallmarks of SOC.

Wetting conditions have a pronounced influence on invasion mechanisms and patterns in porous media<sup>10,12–14</sup>. During the injection of a strongly wetting fluid (i.e. strong imbibition, Fig. 1d–f), the invading fluid advances by coating crevices and corners within the pore space. Slow, constant-rate displacement is achieved by resisting spontaneous imbibition, producing invasion patterns distinct from drainage<sup>13</sup>. However, much like slow drainage, slow strong imbibition evolves via intermittent avalanches<sup>13</sup>. Given the disparity in both pore-scale mechanisms

and macroscopic patterns, it is not obvious that the scale-free features associated with drainage would translate to strong imbibition.

In this paper, we use experiments and simulations to show that slow strong imbibition in porous media exhibits all of the same scale-free features of SOC documented for drainage. In particular, we demonstrate that strong imbibition joins drainage as a second known example to follow the correlation scaling of Furuberg et al.<sup>8</sup> describing the space-time statistics of invasion at the pore scale.

## Results and discussion

**Approach.** Experimentally, we examine fluid-fluid displacement in a micromodel, where cylindrical posts are placed at nodes of an irregular triangular mesh and confined between two transparent disks. Both node locations and post sizes are disordered. The micromodel is fabricated via soft lithography from a photocurable polymer (NOA81, Norland Optical Adhesives)<sup>15,16</sup>, which allows precise control of wettability conditions. We refer to this micromodel design as the benchmark geometry; micromodel characteristics and fabrication details can be found in Zhao et al.<sup>13</sup>. We use fixed contact angles of  $150^\circ \pm 5^\circ$  for drainage and  $7^\circ \pm 3^\circ$  for strong imbibition (Fig. 1), as measured through the invading phase. In both cases, we inject the invading fluid from the center of the micromodel at  $0.4 \mu\text{L min}^{-1}$  while maintaining a constant pressure at the outer perimeter. This slow injection rate provides capillary-dominated flow with negligible viscous effects ( $Ca = 5.8 \times 10^{-3}$ , see Supplementary Methods 1 for details).

Slow fluid-fluid displacement in micromodels can be modeled quasi-statically by incorporating the pore-invasion events of Cieplak and Robbins<sup>17,18</sup> and corner-flow events, as described in detail in Primkulov et al.<sup>19</sup>, and compared against experiments in ref. <sup>20</sup>. In the model, pore-invasion pressures  $p$  are determined from local post geometry and wettability: (i) in slow drainage (Fig. 1b), invasion fills pore bodies in sequence according to the widest available pore throats; (ii) in slow strong imbibition (Fig. 1e), invasion proceeds by sequential post coating. We ran this model in strong imbibition on the benchmark geometry (see Supplementary Methods 2).

**Pore-scale physics and intermittency.** In both drainage and strong imbibition, intermittency emerges from capillary-dominated interactions of the fluid-fluid interfaces with the quenched disorder of the pore geometry. In slow drainage, the invading fluid advances by progressively occupying new pore bodies. Posts act as local pinning sites of the displacement front (Fig. 1). Since viscous forces are negligible, the pressure difference between the two fluids across the interfaces (the Laplace pressure) must be the same for all menisci<sup>19</sup>. As the invading fluid is injected, Laplace pressure builds uniformly across the micromodel until it matches the lowest capillary-entry pressure at the displacement front, at which point the associated meniscus becomes unstable. This meniscus then rapidly advances while all other menisci retract, a process known as a burst event<sup>17,18</sup> or Haines jump<sup>21,22</sup>. These events often occur in rapid successions or avalanches, the sizes of which are scale-free<sup>6</sup>. The repetition of this process generates the marked intermittency of slow drainage, where rapid invasion events are punctuated by periods of apparent inactivity. Since clusters of defending fluid occasionally get surrounded and disconnected (i.e., trapped) during the displacement, the quasi-static invasion process is analogous to invasion percolation with trapping (see Fig. 1 and Table 1).

We find that intermittent pore-scale invasion persists in slow strong imbibition, despite the substantial differences in the pore-scale displacement mechanisms (Fig. 1). In strong imbibition, the invading fluid advances by preferentially coating the corners

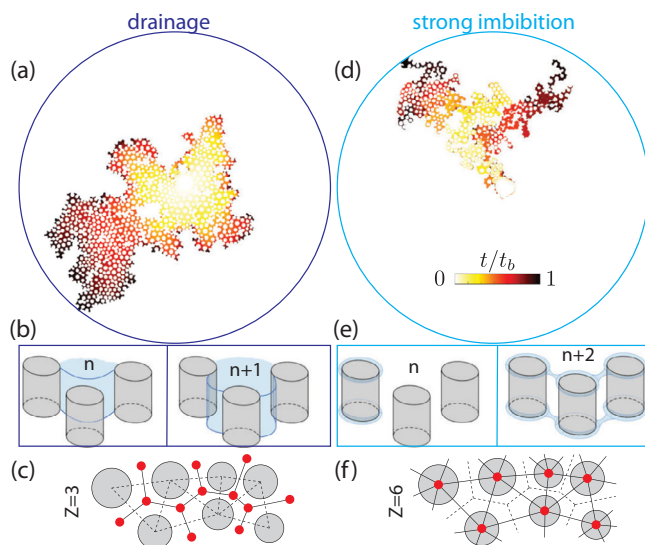


**Fig. 1 Pore-invasion mechanisms.** **a** Temporal evolution of slow fluid-fluid displacement in drainage from experiments in a micromodel patterned with cylindrical posts, where events are colored according to invasion time with  $t_b$  the breakthrough time. Invasion events are intermittent and **b** the invading fluid enters throats with lowest entry pressures and occupies pore bodies. Here, gray cylinders represent posts, the invading fluid is marked in blue, and  $n$  stands for the pore-scale event number. **c** In the quasi-static limit, this process is equivalent to invasion percolation on a hexagonal lattice (coordination number  $Z = 3$ ). Here, red dots and black lines represent network nodes and links, respectively. The dashed lines represent links of a complementary corner-flow network, that is inactive in drainage. **d** Temporal evolution of slow fluid-fluid displacement in strong imbibition from experiments in the same micromodel as **(a)**. Invasion events are intermittent, and **e** the invading fluid advances by coating corners between posts and top/bottom plates, leaving pore bodies filled with defending fluid. **f** In the quasi-static limit, this process is equivalent to invasion percolation on a triangular lattice ( $Z = 6$ ).

**Table 1 Critical exponents for invasion percolation for lattice configurations relevant to our study.**

Lattice	Square	Hexagonal	Triangular
$D_e$	1.22	1.21	1.62
$D$	1.82	1.83	1.89
$\nu$	4/3	4/3	4/3
Trapping	Yes	Yes	No
$a$	[1,1.67]	[1,1.66]	[1,1.86]
$b$	0.74	0.75	0.54

The values of the fractal dimension ( $D$ ), the displacement front fractal dimension  $D_e$ , and the correlation length divergence exponent ( $\nu$ ) are taken from Stauffer and Aharony<sup>33</sup>, Wilkinson and Willemsen<sup>34</sup>, Knackstedt et al.<sup>35</sup>. Values of  $a$  and  $b$  are calculated from Eqs. (2)–(3).

between posts and top/bottom plates<sup>13,19</sup>. After a particular post-coating event, the corner menisci swell as the Laplace pressure increases uniformly across the micromodel until the displacement front touches an uncoated post, triggering rapid coating of the new post<sup>23</sup>. The repetition of this process generates the marked intermittency apparent in experiments (see Supplementary Movie 1). As in drainage, the spatiotemporal evolution of the invasion front displays irregular changes in flow direction and the formation of invasion clusters—a signature of capillary-dominated flow in disordered porous media<sup>24</sup>. Clusters of defending fluid occasionally get surrounded by chains of coated posts, but it remains unclear whether these clusters become disconnected and trapped. Our experimental observations are ambiguous but suggestive of trapping [Supplementary Movie 1], but our simulations do not include trapping because our model does not allow for trapping in strong imbibition<sup>19</sup>. We, therefore, assume that the quasi-static invasion process is analogous to invasion percolation without trapping (Fig. 1 and Table 1). In the Supplementary Note 1, we use a simplified model to show that the presence or absence of trapping does not have significant influence on the invasion statistics.

**SOC signature in waiting time.** Scale-free waiting times between events are a signature of SOC. As a result, the timing of pore-invasion events in drainage is fundamentally unpredictable. To show that post-coating events in strong imbibition also behave in this way, we measure the waiting times between consecutive post-coating events in our experiments. We find that the histogram of waiting times follows a power-law scaling, similar to drainage<sup>6</sup>. The slope of the power-law fit to the experimental data is smaller than 2 (Fig. 2a), confirming that the distribution is scale-free.

**SOC signature in avalanche size.** An avalanche in strong imbibition is a cluster of consecutive post-coating events that originate from the same reference post (e.g., the sequence 88–98 in Fig. 2b). Avalanche size  $\theta$  can be characterized by counting the number of events before encountering a post-coating event disconnected from the cluster (e.g., event 99 in Fig. 2b). For quasi-static invasion, a nearly equivalent definition of  $\theta$  relies on the pressure signal<sup>7,25,26</sup>. Given the lowest capillary entry pressure  $p_0$  at the displacement front at some reference time,  $\theta$  can be defined as the number of pore-invasion events that occur before  $p_0$  is next exceeded (Fig. 2c and ref. 25).

As in drainage<sup>6</sup>, avalanches in strong imbibition retrieved by the counting method detailed in Fig. 2b reveal power-law distributions in both experiments and simulations (Fig. 2d, e). We obtain a similar power-law distribution from the quasi-static pressure signal, a portion of which is illustrated in Fig. 2c. Again, the slope of these power-law distributions is less than 2, indicating that avalanche sizes are scale free. For both drainage

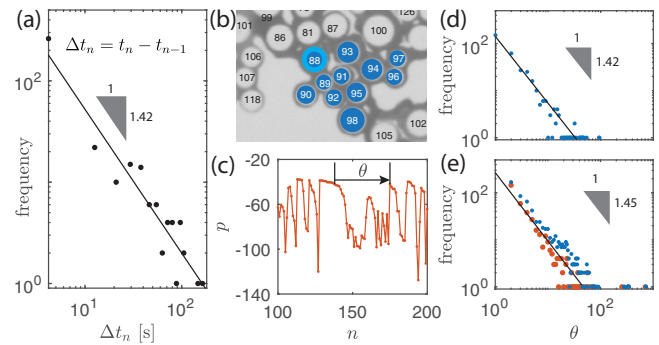


**Fig. 2 SOC features in strong imbibition. a** Scale-free distribution of waiting times between consecutive post-coating events from the strong imbibition experiment (see Supplementary Movie 1). Here, dots represent the histogram data of waiting times, the black line is their least-square fit, and  $n$  stands for the pore-scale event number. We calculate avalanche size  $\theta$  as **b** the cluster size of consecutive events connected to a reference post (e.g., sequence of posts 88–98), or as **c** the number of events found by traversing the pressure signal  $p$  from numerical simulations until a value higher than the reference value is reached. Here, avalanches originate from all data points with negative slope. The distribution of  $\theta$  is scale-free in **d** experiments and **e** simulations, where the colors correspond to  $\theta$ -counting methods in (b, c).

and strong imbibition, the scale-free distribution of avalanches is responsible for the fractal nature of the displacement patterns, which are aggregates of scale-free avalanche clusters. Therefore, slow strong imbibition, despite its distinct invasion mechanism, exhibits all the characteristics of SOC—scale-free waiting times between events, scale-free avalanches, and fractal displacement patterns—that have been documented in slow drainage<sup>6</sup>.

**Furuberg scaling.** The above findings raise the question of whether the correlation scaling of Furuberg et al.<sup>8</sup>, originally proposed for drainage, also holds in strong imbibition. The correlation function  $N(r, n)$  measures the probability of pore invasion at distance  $r$  in space and a number of events  $n$  in time away from a reference event. Here, we measure  $r$  as the Euclidean distance normalized by the characteristic distance between posts, and  $n$  as consecutive pore-scale event number. Furuberg et al.<sup>8</sup> found that in drainage,

$$N(r, n) = r^{-1}f(r^D/n), \quad f(x) \sim \begin{cases} x^a, & x \ll 1 \\ x^{-b}, & x \gg 1 \end{cases} \quad (1)$$

where  $D$  is the fractal dimension of the displacement pattern. For slow drainage, Furuberg et al.<sup>8</sup> obtained exponents  $a \approx 1.4$  and  $b \approx 0.6$  by fitting the results of an invasion-percolation model. Roux and Guyon<sup>25</sup> argued that  $a$  and  $b$  are linked to exponents of ordinary percolation theory, and Maslov<sup>26</sup> subsequently showed that, under that ansatz,

$$b = 1 - (D_e - 1/\nu)/D, \quad (2)$$

where  $D_e$  is the fractal dimension of the fluid-fluid interface and  $\nu$  is the correlation-length-divergence exponent from ordinary percolation. Roux and Guyon<sup>25</sup> argued that  $a \geq 1$ , while Moura et al.<sup>7</sup> showed that  $a = 1 + D_e/D$  when  $n \gg 1$ , so we should expect

$$1 \leq a \leq 1 + D_e/D. \quad (3)$$

Expected values of exponents  $a$  and  $b$  from Eqs. (2) and (3) are reported in Table 1. Equation (1) was only recently verified experimentally in drainage by Moura et al.<sup>7</sup>.

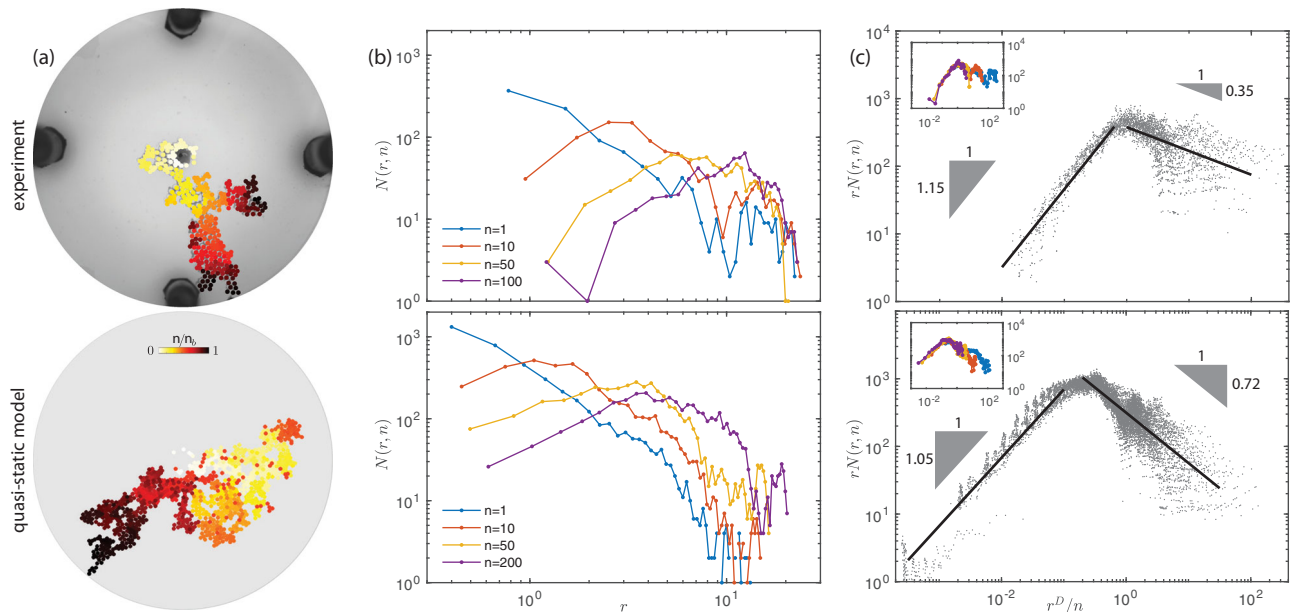


**Fig. 3 Spatiotemporal correlation scaling of post-coating events.** Verification of Eq. (1) in slow strong imbibition for our experiment and model. **a** Invasion-event-number plot, where events are colored by event number  $n$  with  $n_b$ , the number of events at breakthrough. **b** Plots of  $N(r, n)$  vs.  $r$  for several values of  $n$ . Here,  $N$ ,  $r$ , and  $n$  are correlation function, distance, and event number, respectively. **c** Collapse of  $rN(r, n)$  vs.  $r^D/n$  points to the validity of the scaling in Eq. (1). Here, data points correspond to all different values of the time delay  $n$ , while the insets show the collapse for a selection of  $n$  from (b). The black lines represent the least-square fit of the data.

**Table 2 Result of data collapse analogous to Fig. 3c for simulations on the benchmark geometry, and also on a set of regular lattices with post radii assigned from a uniform distribution.**

	Exponents	Drainage $\theta = 150^\circ$	Strong imbibition $\theta = 7^\circ$
Benchmark geometry	$a$	1.21	1.05
	$b$	0.58	0.72
Regular lattice, random radii	$a$	$1.41 \pm 0.08$	$1.11 \pm 0.06$
	$b$	$0.72 \pm 0.15$	$0.76 \pm 0.13$

We report the mean and the standard deviation from 40 realizations.

**Furuberg scaling in strong imbibition.** Both model and experiment allow us to test the validity of Eq. (1) in strong imbibition (Fig. 3a). For a fixed value of  $n$ ,  $N(r, n)$  is the histogram of distances  $r$  between pore-scale events separated in time by  $n$  events (Fig. 3b). The data from our model and experiments resemble those reported for strong drainage<sup>7,8</sup>, with peaks in  $N(r, n)$  moving to larger  $r$  as  $n$  increases. These data collapse for both model and experiment when we plot  $rN(r, n)$  against  $r^D/n$  (Fig. 3c), with a peak near  $r^D/n = 1$  and power-law behavior on either side of the peak signifying the validity of Eq. (1) in strong imbibition.

We confirm the robustness of this collapse by running a set of additional simulations for both drainage and strong imbibition in which we place posts on a regular triangular lattice and draw post radii from a uniform distribution; the resulting data also collapses, as in Fig. 3, with values of exponents  $a$  and  $b$  reported in Table 2.

Roux and Guyon<sup>25</sup> demonstrated that the robustness of the collapse suggested by Eq. (1) relies on the power-law distributions of avalanches ( $P_n(\theta) \sim \theta^{-\tau_b}$ ) and distances between active pores at the displacement front ( $Q_\theta(r) \sim r^\alpha$ ). These conditions are satisfied in both drainage and strong imbibition, where fluid displacement exhibits features of SOC. However, the predictions of Eqs. (2) and (3) for the slopes  $a$  and  $b$  appear not to hold in strong imbibition, with the expected value of  $b$  (Table 1) significantly different from the value in the experiment (Fig. 3c)

and almost two standard deviations away from the mean value in simulations (Table 2). In fact, Biswas et al.<sup>9</sup> showed that  $\tau_b$  is sensitive to the details of the pore structure and the presence of spatial correlation, something that the relatively wide standard deviation across our simulations also shows. This dependence is absent from Eq. (2), where  $b$  (which is a function of  $\tau_b$ <sup>25</sup>) depends only on  $\nu$  and fractal dimensions.

**Conclusions.** We have demonstrated that slow fluid-fluid displacement in strong imbibition exhibits features of SOC previously documented for drainage. The invading fluid advances intermittently, and scale-free distributions emerge for waiting times and avalanche sizes. Both our model and our experiment also show that avalanches in strong imbibition robustly follow the pore-scale event correlation of Furuberg et al.<sup>8</sup> Slow drainage and strong imbibition are thus the only two known examples of SOC that follow a definitive correlation of events in space and time [Eq. (1)]. It is surprising that these two phenomena—governed by entirely distinct pore-level mechanisms—both exhibit collapse in the correlated nature of invasion percolation.

Furthermore, we anticipate that the correlation scaling of Furuberg et al.<sup>8</sup> would still be valid in 3D, as long as the two assumptions of Roux and Guyon<sup>25</sup> (power-law scaling of avalanche sizes and distance between active pores) still hold. Validating this correlation scaling in 3D with either simulations

or experiments would be an intriguing next step. Additionally, we found that increasingly strong spatial correlation in wettability or pore-sizes eventually breaks the collapse of the correlation data (Fig. 3c). This is especially true in weak imbibition, where the invasion dynamics on a highly correlated regular lattice resembles the growth of a crystal<sup>27</sup>. While this discussion falls outside the scope of this letter, it is another great direction for follow-up studies.

Scientific understanding of SOC is still at a relatively early stage<sup>1,28,29</sup>, and much of the progress in the field is made by studying one example of SOC and trying to extrapolate to others<sup>30</sup>. Many other natural examples of SOC, like landslides, snow avalanches, and earthquakes, share features similar to avalanches in drainage and strong imbibition<sup>1</sup>. For instance, in earthquakes: (i) the sliding of geologic faults occurs by means of intermittent stick-slip motion; (ii) magnitudes and waiting times between consecutive earthquakes are scale-free<sup>1</sup>, and (iii) earthquake locations within slip planes have been speculated to form fractal patterns<sup>4</sup>. An intriguing follow-up to this work would be to investigate whether the scaling in Eq. (1) holds for earthquakes, given the density and precision of modern earthquake catalogs<sup>31,32</sup>.

### Data availability

All relevant data are available upon reasonable request from the corresponding author.

### Code availability

A detailed description of the quasi-static model used in this study has been published in Primkulov et al.<sup>19</sup>. All the algorithmic details needed to reproduce the results of the numerical simulations are provided in that publication.

Received: 3 October 2021; Accepted: 4 February 2022;

Published online: 11 March 2022

### References

- Bak, P. *How Nature Works: the Science of Self-Organized Criticality* (Springer Science & Business Media, 2013).
- Bak, P., Tang, C. & Wiesenfeld, K. Self-organized criticality: an explanation of the  $1/f$  noise. *Phys. Rev. Lett.* **59**, 381 (1987).
- Bak, P., Tang, C. & Wiesenfeld, K. Self-organized criticality. *Phys. Rev. A* **38**, 364 (1988).
- Bak, P. & Chen, K. The physics of fractals. *Phys. D: Nonlinear Phenom.* **38**, 5 (1989).
- Martys, N., Robbins, M. O. & Cieplak, M. Scaling relations for interface motion through disordered media: application to two-dimensional fluid invasion. *Phys. Rev. B* **44**, 12294 (1991).
- Moura, M., Måløy, K. J. & Toussaint, R. Critical behavior in porous media flow. *EPL* **118**, 14004 (2017).
- Moura, M., Måløy, K. J., Flekkøy, E. G. & Toussaint, R. Verification of a dynamic scaling for the pair correlation function during the slow drainage of a porous medium. *Phys. Rev. Lett.* **119**, 154503 (2017).
- Furuberg, L., Feder, J., Aharony, A. & Jøssang, T. Dynamics of invasion percolation. *Phys. Rev. Lett.* **61**, 2117 (1988).
- Biswas, S., Fantinel, P., Borgman, O., Holtzman, R. & Goehring, L. Drying and percolation in correlated porous media. *Phys. Rev. Fluids* **3**, 124307 (2018).
- Lenormand, R., Zarcone, C. & Sarr, A. Mechanisms of the displacement of one fluid by another in a network of capillary ducts. *J. Fluid Mech.* **135**, 337 (1983).
- Måløy, K. J., Furuberg, L., Feder, J. & Jøssang, T. Dynamics of slow drainage in porous media. *Phys. Rev. Lett.* **68**, 2161 (1992).
- Blunt, M. J. & Scher, H. Pore-level modeling of wetting. *Phys. Rev. E* **52**, 6387 (1995).
- Zhao, B., MacMinn, C. W. & Juanes, R. Wettability control on multiphase flow in patterned microfluidics. *Proc. Natl Acad. Sci. USA* **113**, 10251 (2016).
- Odier, C., Levaché, B., Santanach-Carreras, E. & Bartolo, D. Forced imbibition in porous media: a fourfold scenario. *Phys. Rev. Lett.* **119**, 208005 (2017).
- Bartolo, D., Degré, G., Nghe, P. & Studer, V. Microfluidic stickers. *Lab a Chip* **8**, 274 (2008).

- Levaché, B., Azioune, A., Bourrel, M., Studer, V. & Bartolo, D. Engineering the surface properties of microfluidic stickers. *Lab Chip* **12**, 3028 (2012).
- Cieplak, M. & Robbins, M. O. Dynamical transition in quasistatic fluid invasion in porous media. *Phys. Rev. Lett.* **60**, 2042 (1988).
- Cieplak, M. & Robbins, M. O. Influence of contact angle on quasistatic fluid invasion of porous media. *Phys. Rev. B* **41**, 11508 (1990).
- Primkulov, B. K. et al. Quasistatic fluid-fluid displacement in porous media: Invasion-percolation through a wetting transition. *Phys. Rev. Fluids* **3**, 104001 (2018).
- Zhao, B. et al. Comprehensive comparison of pore-scale models for multiphase flow in porous media. *Proc. Natl Acad. Sci. USA* **116**, 13799 (2019).
- Haines, W. B. Studies in the physical properties of soil. V. The hysteresis effect in capillary properties, and the modes of moisture distribution associated therewith. *J. Agric. Sci.* **20**, 97 (1930).
- Berg, S. et al. Real-time 3D imaging of Haines jumps in porous media flow. *Proc. Natl Acad. Sci. USA* **110**, 3755 (2013).
- Ponomarenko, A., Quéré, D. D. & Clanet, C. A universal law for capillary rise in corners. *J. Fluid Mech.* **666**, 146 (2011).
- Primkulov, B. K. et al. Wettability and Lenormand's diagram. *J. Fluid Mech.* **923**, A34 (2021).
- Roux, S. & Guyon, E. Temporal development of invasion percolation. *J. Phys. A: Math. Gen.* **22**, 3693 (1989).
- Maslov, S. Time directed avalanches in invasion models. *Phys. Rev. Lett.* **74**, 562 (1995).
- Lenormand, R. Liquids in porous media. *J. Phys.: Condens. Matter* **2**, SA79 (1990).
- Yang, X., Du, S. & Ma, J. Do earthquakes exhibit self-organized criticality? *Phys. Rev. Lett.* **92**, 228501 (2004).
- Marković, D. & Gros, C. Power laws and self-organized criticality in theory and nature. *Phys. Rep.* **536**, 41 (2014).
- Goldenfeld, N. & Kadanoff, L. P. Simple lessons from complexity. *Science* **284**, 87 (1999).
- DeVries, P. M. R., Viégas, F., Wattenberg, M. & Meade, B. J. Deep learning of aftershock patterns following large earthquakes. *Nature* **560**, 632 (2018).
- Ross, Z. E., Trugman, D. T., Hauksson, E. & Shearer, P. M. Searching for hidden earthquakes in Southern California. *Science* **364**, 767 (2019)..
- Stauffer, D. & Aharony, A. *Introduction to Percolation Theory*, <https://doi.org/10.4324/9780203211595> (Taylor & Francis Group, 1985).
- Wilkinson, D. & Willemsen, J. F. Invasion percolation: a new form of percolation theory. *J. Phys. A: Math. Gen.* **16**, 3365 (1983).
- Knackstedt, M. A., Sahimi, M. & Sheppard, A. P. Nonuniversality of invasion percolation in two-dimensional systems. *Phys. Rev. E* **65**, 035101 (2002).

### Acknowledgements

This work was funded by the KFUPM-MIT collaborative agreement "Multiscale Reservoir Science". R.J. acknowledges funding from the US Department of Energy (grant DE-SC0018357).

### Author contributions

R.J. designed the research. B.K.P. carried out the analysis of the experimental data and numerical simulations. B.Z. had previously conducted the laboratory experiments. B.K.P., B.Z., C.W.M., and R.J. discussed the results. B.K.P. led the writing, and B.Z., C.W.M., and R.J. participated in writing and reviewing the manuscript.

### Competing interests

The authors declare no competing interest.

### Additional information

**Supplementary information** The online version contains supplementary material available at <https://doi.org/10.1038/s42005-022-00826-1>.

**Correspondence** and requests for materials should be addressed to Ruben Juanes.

**Peer review information** *Communications Physics* thanks Marcel Moura, Renaud Toussaint and the other, anonymous, reviewer(s) for their contribution to the peer review of this work. Peer reviewer reports are available.

**Reprints and permission information** is available at <http://www.nature.com/reprints>

**Publisher's note** Springer Nature remains neutral with regard to jurisdictional claims in published maps and institutional affiliations.



**Open Access** This article is licensed under a Creative Commons Attribution 4.0 International License, which permits use, sharing, adaptation, distribution and reproduction in any medium or format, as long as you give appropriate credit to the original author(s) and the source, provide a link to the Creative Commons license, and indicate if changes were made. The images or other third party material in this article are included in the article's Creative Commons license, unless indicated otherwise in a credit line to the material. If material is not included in the article's Creative Commons license and your intended use is not permitted by statutory regulation or exceeds the permitted use, you will need to obtain permission directly from the copyright holder. To view a copy of this license, visit <http://creativecommons.org/licenses/by/4.0/>.

© The Author(s) 2022